

Stratospheric Final Warmings fall into two categories with different evolution over the course of the year

Alain Hauchecorne, Chantal Claud, Philippe Keckhut, Alexis Mariaccia

▶ **To cite this version:**

Alain Hauchecorne, Chantal Claud, Philippe Keckhut, Alexis Mariaccia. Stratospheric Final Warmings fall into two categories with different evolution over the course of the year. Communications Earth & Environment, 2022, 3, pp.4. 10.1038/s43247-021-00335-z . insu-03527231

HAL Id: insu-03527231

https://insu.hal.science/insu-03527231

Submitted on 15 Jan 2022

HAL is a multi-disciplinary open access archive for the deposit and dissemination of scientific research documents, whether they are published or not. The documents may come from teaching and research institutions in France or abroad, or from public or private research centers.

L'archive ouverte pluridisciplinaire **HAL**, est destinée au dépôt et à la diffusion de documents scientifiques de niveau recherche, publiés ou non, émanant des établissements d'enseignement et de recherche français ou étrangers, des laboratoires publics ou privés.



Distributed under a Creative Commons Attribution 4.0 International License

communications earth & environment

ARTICLE

https://doi.org/10.1038/s43247-021-00335-z OPEN

Stratospheric Final Warmings fall into two categories with different evolution over the course of the year

Alain Hauchecorne [1✉], Chantal Claud[2], Philippe Keckhut[1] & Alexis Mariaccia[1]

In early spring the stratospheric zonal circulation reverses from westerly to easterly. The transition, called Stratospheric Final Warming (SFW), may be smooth and late, mainly controlled by the solar radiative heating of the polar region, or early and abrupt with rapid increase of polar temperature and deceleration of the zonal wind, forced by the planetary wave activity. Here we present a study, based on 71 years meteorological reanalysis data. Two composites of radiative and dynamical SFWs have been built. There is a very significant difference in the evolution during the year of polar temperature and 60°N zonal wind between the two composites. The state of the polar vortex on given month is anticorrelated with its state 2 to 3 months earlier. Early winter is anticorrelated with mid-winter and mid-winter with late winter/early spring. The summer stratosphere keeps a memory of its state in April–May after the SFW until late June.

[1] Université de Versailles Saint-Quentin-en-Yvelines, Université Paris-Saclay, Sorbonne Université (SU), CNRS, LATMOS, 11 Boulevard d'Alembert, 78280 Guyancourt, France. [2] Ecole Polytechnique, CNRS, Laboratoire de Météorologie Dynamique, 91128 Palaiseau, Cedex, France.
✉email: alain.hauchecorne@latmos.ipsl.fr

Sudden Stratospheric Warming (SSW) events are the most spectacular dynamic events that occur in the middle atmosphere (stratosphere and mesosphere). The stratospheric polar temperature can increase in one or two weeks by several tens of degrees in mid-winter. According to the World Metorological Organization[1], an SSW is called major if the stratospheric zonal circulation reverses from west to east at 60°N-10 hPa, similar to summer circulation[2–7]. SSWs are forced by the propagation and upward amplification of planetary waves (PWs). PWs are generated by thermal contrasts between the continents and the oceans and the flow over the orography[8]. SSWs appear to play a major role not only on the variability of stratospheric composition, affecting the polar vortex where ozone depletion occurs, but also on the impact of the stratosphere on tropospheric circulation and ground weather[9,10]. The pressure-temperature perturbations of the polar region at 10 hPa, characterized by weak polar vortex events (corresponding to SSWs) and strong polar vortex events, propagates downwards to the surface within about one month[11]. There is a growing interest in the study of dynamical coupling between the stratosphere and the troposphere during SSW events due to the potential to improve sub-seasonal to seasonal weather predictions[12–14]. Climate model systems are able to predict the occurrence of SSW up to two weeks in advance[15–18]. Major SSW events are often preceded by one or several minor SSWs characterized by peaks of warming in the middle and upper polar stratosphere but without zonal wind reversal[6]. The temperature of the Arctic stratosphere during the spring is controlled by the intensity of midwinter planetary wave activity, a strong (weak) midwinter forcing leading to a warmer (colder) spring Artic temperature[19]. This suggests that there is a preconditioning of the stratosphere to favour the occurrence of SSW events and that the state of the stratosphere in a given month in winter is depending on its state during the previous months[20,21].

In spring the solar radiation begins to warm the polar stratospheric region, causing the polar vortex to collapse[22] and the summertime polar anticyclone surrounded by easterly winds to establish. The transition from westerly to easterly circulation, called Stratospheric Final Warming (SFW), may be late and very smooth, guided mainly by radiative processes, or very abrupt, preceded by an amplification of planetary waves and a strong temperature peak similar to a mid-winter SSW[5,6]. SFWs are generally classified in the literature according to their timing in early and late SFWs[23,24]. In this study we prefer to classify the SFWs according to their nature in radiative and dynamical SFWs. The timing of SFWs has been first studied in the context of the Artic ozone depletion and the persistence of the polar vortex is highly correlated with the heat flux during the two months before its breakup[25,26]. There is a strong stratosphere-troposphere coupling during the stratospheric wind reversal with a North Atlantic Oscillation like pattern in the near surface geopotential field[27] and a concomitant tropospheric wind deceleration[28]. The timing of SFWs is related to the occurrence of SSWs. Early SFWs occur preferentially in years without SSW and there is a higher probability of a late SFW if an SSW occurs in January-February[23]. Early SFWs are more strongly driven by wave forcing and are less predicted than late SFW. A significant increased predictive skill of NH near-surface temperature anomalies is obtained only for early SFWs[24].

The objectives of this paper are to better characterize SFW events according to their nature and their date of occurrence, and to explore the seasonal memory of the stratosphere in relation with mid-winter SSW and SFW events. This study is based on 71 years of ERA5 reanalysis recently extended backward to 1950[29].

Results

In order to study the behaviour of SFWs we define for each year the following quantities:

- The SFW date is defined as the day of the final reversal of the zonal wind at 60°N, 10 hPa smoothed over 5 days.
- The SFW temperature anomaly is taken as the maximum of polar temperature anomaly from 7 days before to 7 days after the wind reversal. The definition of the temperature anomaly is defined in the methods section.
- The SFW wave 1 amplitude is taken as the maximum amplitude of geopotential wave 1 and 2 at 60°N, 10 hPa from 7 days before to 7 days after the inversion day.
- The zonal mean meridional heat flux defined as:

$$\overline{v'T'}$$

where v' and T' are the deviation from the zonal mean respectively of the meridional wind and the temperature. The heat flux is computed at 60°N-10 hPa during 14 days before to the reversal day.

The date of the SFW varies between day 66 (5 March 2016) and day 131 (11 May 1981) and the SFW temperature anomaly varies between −3.8 K (in 1999) and +24.7 K (in 2016) (Fig. 1a). It is difficult to detect a trend in these series. Negative temperature anomalies can be explained by the fact that the date of the final warming is defined by the final zonal wind reversal, not by an increase in polar temperature. In the case of late radiative warming, the polar temperature is not increased by wave activity and the temperature may be lower than the climatology that includes the years with more wave activity. During the period 1997–2010 the SFW dates were later and the temperature anomalies were smaller but the reverse was true after 2010 (respectively day 113 vs day 101 and 1.6 K vs 7.4 K in average). Recent studies using CMIP5/6 simulations have shown that possible changes in the timing and intensity of SFWs may occur in relation with the global climate change[22]. There is a clear anticorrelation between the date of the SFW and the temperature anomaly (Fig. 1b; correlation coefficient = −0.88). This suggests that SFWs can be separated into two categories, the dynamical SFWs with a peak of warming similar to SSWs occurring earlier in the season and the radiative SFWs occurring later with a smooth transition to the summer season. Figure 2a shows the high correlation ($R = 0.885$) between the of geopotential wave 1 amplitude and the temperature anomaly during the SFW. It confirms that high temperature anomalies are caused by high planetary wave activity[30]. The zonal-mean heat flux is often used to estimate the planetary wave activity that propagates from the troposphere to the stratosphere[31]. The temperature anomaly is also highly correlated with the mean vertical heat flux during the two weeks before the wind reversal day (Fig. 2b). We conclude that the polar temperature anomaly is a good proxy to classify SFWs according to the dominant forcing (radiative or dynamic). To better understand the difference between SFWs associated with high and low temperature anomalies, two composites were constructed, the dynamic composite including all years with an anomaly >10 K (20 samples) and a radiative composite including all years with an anomaly <0 K (20 samples). Using this classification, all SFWs belonging to the radiative composite correspond to a low heat flux (<24 Kms^{-1}). On the contrary all SFWs belonging to the dynamical composite correspond to a strong heat flux (>40 Kms^{-1}).

The polar temperature and the zonal wind evolution during the year are very different between the two composites as shown in Fig. 3. For the dynamical composite we observe a relatively strong vortex in February with low temperature and high zonal wind, a peak of warming in late March- early April with an early reversal of the zonal wind. For the radiative composite we observe a peak of warming in February with a deceleration of the zonal wind, a relatively cold temperature in March and a smooth transition to easterly wind at the end of April. It means that the nature of the SFW is related to the evolution of the polar vortex during the preceding winter. These results are in agreement with published results[23]

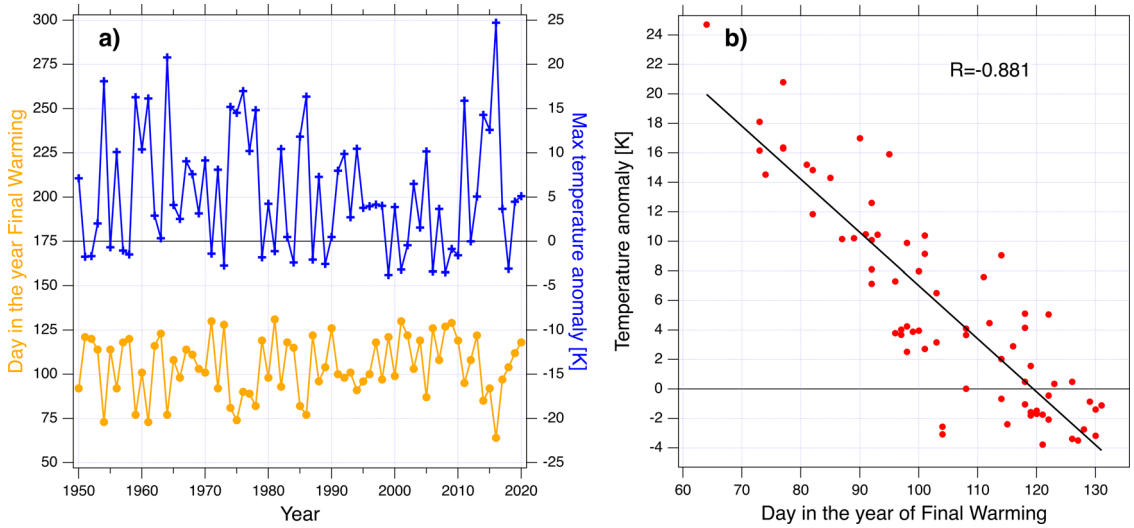


Fig. 1 FSW date and temperature anomaly. a Final warming day (in light orange, left scale) and final warming temperature anomaly (in dark blue, right scale). **b** Correlation between the final warming day in the year and the polar temperature anomaly. The black line represents the linear regression (correlation coefficient $R = -0.881$).

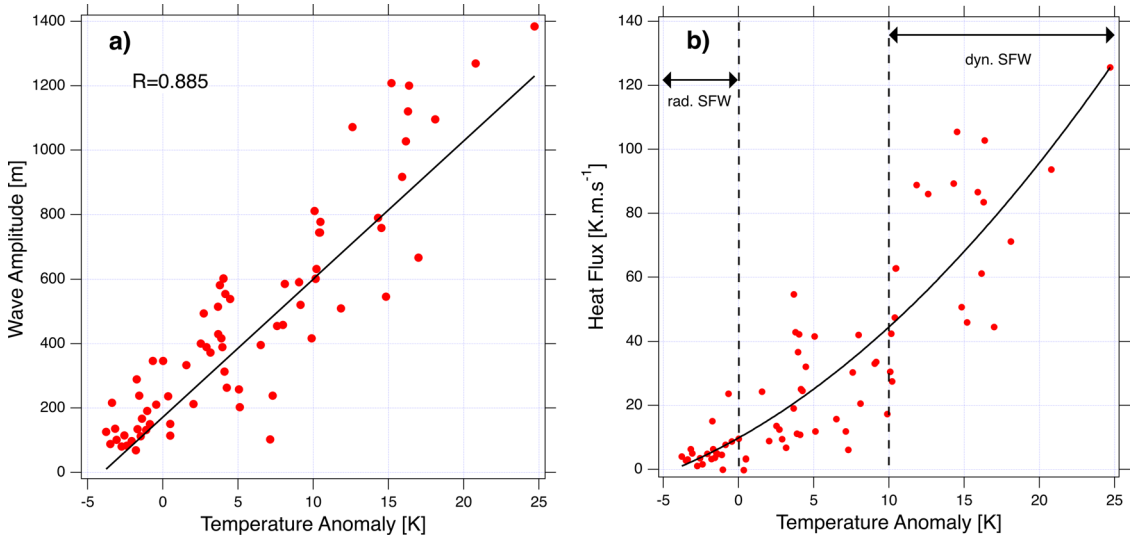


Fig. 2 FSW wave amplitude, heat flux and temperature anomaly. a Amplitude of geopotential wave 1 at 60°N-10 hPa versus final warming temperature anomaly and linear fit. The black line represents the linear regression (correlation coefficient $R = 0.885$). **b** Zonal-mean heat flux at 60°N-10 hPa versus temperature anomaly. The black line represents the parabolic fit.

showing that early SFWs tend to be preceded by non-SSW winters, while late spring SFWs are mostly preceded by SSW events in midwinter. The difference between the two composites in polar temperature and zonal wind persists during the summer until at least end of June. The differences between the mean values of the two composites are highly significant, well beyond the 95% confidence levels, in February in one direction and from late March to early May in the opposite direction for both zonal wind and temperature anomalies. These results indicate that the state of the stratosphere at a given time is depending on its state during the 2–3 previous months. We can say that there is a memory of the stratosphere[12].

To test the hypothesis of a memory of the stratosphere, the time-lag correlation between monthly mean anomalies in 60°N zonal wind and polar temperature are presented in Fig. 4. Data series are first detrended before computing the correlations to avoid a perturbation by long-term linear trends.

The polar temperature between two successive months is correlated at 95% confidence level in early winter (October to December) and in spring-summer (April to July) (Fig. 4a). From mid-winter to early spring, we observe an anticorrelation for a 2 to 3-month time lag (between January and March, February and April–May, March and May–June). The zonal wind between two successive months is systematically correlated at 95% confidence level except between February and March (Fig. 4b). A significant anticorrelation is observed for a 2 to 4 months lag between January and March, February and April–June, March and May–July. The proposed interpretation is the decrease of planetary wave activity after an SSW that allows the zonal wind to reaccelerate and the polar region to cool. For both the zonal wind and the polar temperature the summer months (June to August) are correlated between them. This indicates that there is a memory of the summer polar stratosphere after the SFW.

As expected, a systematic anticorrelation at 95% confidence level is observed between the 60°N zonal wind and the polar temperature for the same month (Fig. 4c), a stronger vortex

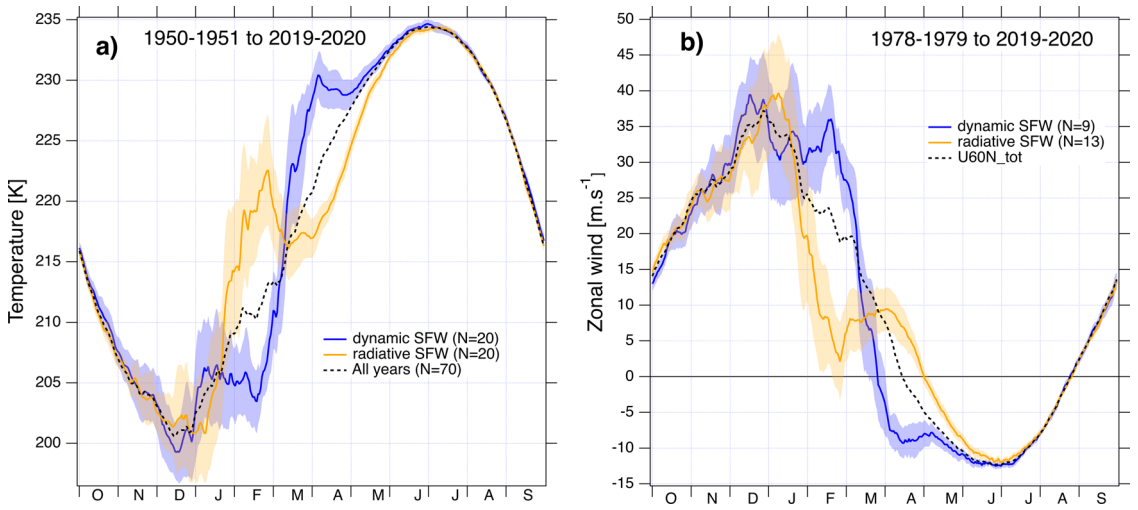


Fig. 3 Polar temperature and zonal wind evolution for the two composites. a Evolution of the polar temperature and, **b** of the 60°N zonal wind (for the two SFW composites with 20 dynamical SFWs (in dark blue) and 20 radiative SFWs (in light orange). The shaded area represents the 95% confidence level (2 standard deviations) on the mean values. The dashed black line represents the evolution averaged over the 70 years.

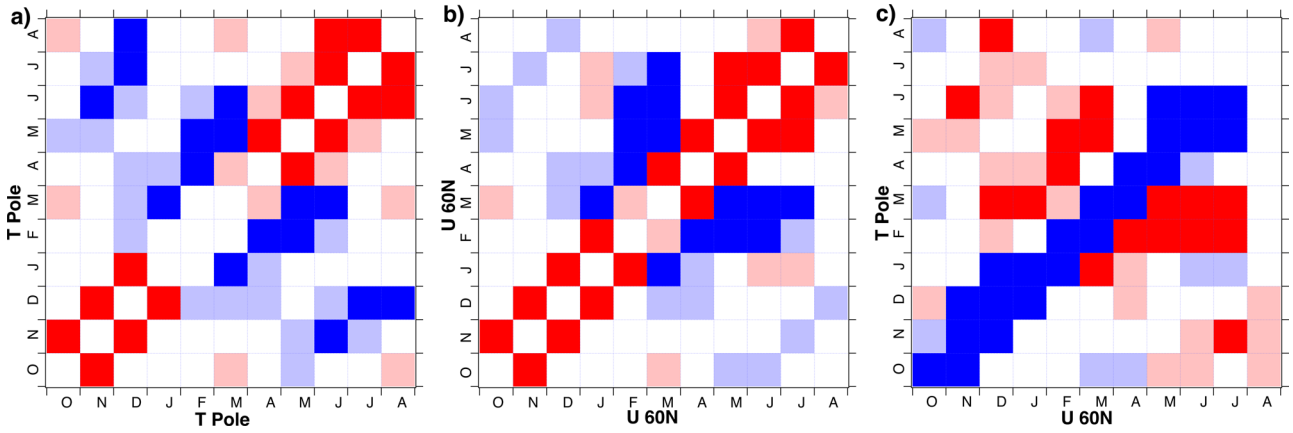


Fig. 4 Correlation between the polar temperature and the zonal wind. Confidence level of the correlation between the monthly mean values of 2 months of the year for: **a** temperature-temperature, **b** wind-wind and **c** temperature-wind correlations. +1 to +2 SD (standard deviation) light red, >+2 SD dark red, −2 to −1 SD light blue, <−2 SD dark blue. For correlation between two months of the same variable (Fig. 4a, b), the diagonal is left blank and the figure is symmetrical in relation to the diagonal.

corresponding to a faster zonal wind and a colder polar temperature. The correlation persists for some months for a time difference of one month between the two data series. A significant correlation is observed between the zonal wind for a given month from December to March and the polar temperature 2–3 months later. When the zonal wind blows faster, the planetary wave activity can increase and drive an SSW during the later months.

Conclusions. The analysis of 71 years ERA5 data from 1950 to 2020 allowed us to characterize the seasonal evolution of the polar stratosphere in relation with mid-winter SSWs and SFWs. The main conclusions are:

(1) The state of the polar vortex on given month, characterized by the polar temperature and the 60°N zonal wind anomalies, is anticorrelated with its state 2–3 months earlier. Early winter is anticorrelated with mid-winter and mid-winter is anticorrelated with late winter/early spring. This anticorrelation may be explained by the decrease of planetary wave activity after an SSW that tends to cool the polar region and accelerate the zonal wind around it.

(2) SFWs may be classified in two categories, the dynamical and early SFWs similar to mid-winter SSWs with a strong positive polar temperature anomaly and the radiative and late SFWs without positive temperature anomaly. There is a very significant difference in the evolution of both polar temperature and zonal wind during the winter between the radiative and dynamical SFW composites. The polar region is colder with a stronger zonal wind in February and warmer with a weaker zonal wind from late March to early May in the dynamical composite compared to the radiative one.

(3) The summer stratosphere (polar temperature and 60°N zonal wind) keeps a memory of its state in April–May after the SFW until at least July. The polar region is warmer with a stronger easterly wind after a dynamical SFW.

Methods

ERA5 climate reanalysis, produced by the European Center for Medium-range Weather Forecasts (ECMWF), covers the period from 1950 to now since the recent extension to the period pre-satellite period 1950–1978. ERA5 data are available on 37 pressure levels from 1000 hPa to 1 hPa with an hourly time resolution and a horizontal resolution down to 0.25° in latitude and longitude. In the present study, we used daily data at 12 UT on the 4 pressure levels 10, 20, 30 and 50 hPa with a

2.5° × 2.5° latitude-longitude grids. We use the dataset ERA5.1 for the period 2000–2006 to correct the cold bias in ERA5 stratospheric data during this period[32].

To follow the evolution of the polar stratosphere daily quantities are computed:

- Zonal wind at 60°N-10 hPa
- Polar temperature averaged over 80–90°N and 50-10 hPa
- Amplitude of geopotential wave 1 at 60°N-10 hPa
- Zonal-mean meridional heat flux averaged over 45–75°N at 10 hPa

The 71-year climatology of the zonal wind and polar temperature is calculated and the anomaly of these quantities is obtained by subtracting the climatology for the same day of the year.

Data availability

The polar stratospheric daily quantities used in this study are freely available in HDF5 format on https://zenodo.org/record/5744919#.YaZUW_HMJBw. Data underlying the Figs. 1–4 are in Supplementary Data 1–4 Excel files.

Received: 21 May 2021; Accepted: 17 December 2021;
Published online: 10 January 2022

References

1. McInturff, R. M., Ed. Stratospheric warmings: Synoptic, dynamic and general-circulation aspects. *NASA Reference Publ.* NASA-RP-1017, 174. http://ntrs.nasa.gov/archive/nasa/casi.ntrs.nasa.gov/19780010687.pdf. (1978).
2. Matsuno, T. A dynamical model of the stratospheric sudden warming. *J. Atmos. Sci.* **28**, 1479–1494 (1971).
3. Labitzke, K. Stratospheric-mesospheric midwinter disturbances: a summary of observed characteristics. *J. Geophys. Res.* **86**, 9665–9678 (1981).
4. Charlton-Perez, A. J. & Polvani, L. A new look at stratospheric sudden warmings. Part I: climatology and modelling benchmarks. *J. Climate,* **20**, 449–469 (2007).
5. Butler, A. H. et al. Match defining sudden stratospheric warmings. *Bull. Amer. Meteor. Soc.* **96**, 1913–1928 (2015).
6. Maury, P., Claud, C., Manzini, E., Hauchecorne, A. & Keckhut, P. Characteristics of stratospheric warming events during Northern winter. *J. Geophys. Res. Atmos.* **121**, 5368–5380 (2016).
7. Baldwin et al. Sudden Stratospheric Warmings. *Rev. Geophys.* **59**, 1–37 (2020).
8. Charney, J. G. & Drazin, P. G. Propagation of planetary-scale disturbances from the lower into the upper atmosphere. *J. Geophys. Res.* **66**, 83–109 (1961).
9. Cohen, J. & Jones, J. Tropospheric precursors and stratospheric warmings. *J. Clim.* **24,**, 6562–6572 (2011).
10. Ineson et al. Solar forcing of winter climate variability in the Northern Hemisphere. *Nat. Geosci.* **4**, 753–757 (2011).
11. Baldwin, M. & Dunkerton, T. Stratospheric harbingers of anomalous weather regimes. *Science* **294**, 581–584 (2001).
12. Baldwin, M. et al. Stratospheric memory and skill of extended-range weather forecasts. *Science* **301**, 636–640 (2003).
13. Scaife, A. A. et al. Seasonal winter forecasts and the stratosphere. *Atmos. Sci. Lett.* **17**, 51–56 (2015).
14. Domeisen et al. The role of the stratosphere in subseasonal to seasonal prediction: 1. Predictability of the stratosphere,. *J. Geophys. Res. Atmos.* **125**, 2019JD030920 (2020).
15. Rao, J. et al. The stratospheric sudden warming event in February 2018 and its prediction by a climate system model, 2018. *J. Geophys. Res. Atmos.* **123**. https://doi.org/10.1029/2018JD028908 (2018).
16. Taguchi, M. Comparison of subseasonal-to-seasonal model forecasts formajor stratospheric sudden warmings. J. *Geophys. Res. Atmos.* **123**, 10231–10247.
17. Karpechko, A. Y. Predicting sudden stratospheric warming 2018 and its climate impacts with a multimodel ensemble. *Geophys. Res. Lett.* **45**, 13, 538–13,546 (2018).
18. Rao, J. The 2019 new year stratospheric sudden warming and its rea-time predictions in multiple S2S models,. *J. Geoph. Res. Atmos.* **124**, 11155–11174 (2019).
19. Newman, P. A., Nash, A. R. & Rosenfield, J. E. What controls the temperature of the Arctic stratosphere during the spring? *J. Geophys. Res. Atmos.* **106**, 19999–20010 (2001).
20. Angot, G., Keckhut, P., Hauchecorne, A. & Claud, C. Contribution of stratospheric warmings to temperature trends in the middle atmosphere from the lidar series obtained at Haute-Provence Observatory (44°N), *J. Geoph. Res. Atmos.* **117**, D21102 (2012).
21. Bancalá, S., Krüger, K. & Giorgetta, M. The preconditioning of major sudden stratospheric warmings. *J. Geophys. Res.* **117**, D04101 (2012).
22. Rao, J. & Garfinkel, C. I. Projected changes of stratospheric final warmings in the Northern and Southern Hemispheres by CMIP5/6 models. *Clim. Dyn.* **56**, 3353–3371 (2021).
23. Hu, J. G., Ren, R. C. & Xu, H. M. Occurrence of winter stratospheric sudden warming events and the seasonal timing of spring stratospheric final warming. *J. Atmos. Sci.* **71**, 2319–2334 (2014).
24. Butler, A. H. et al. Predictability of Northern Hemisphere final stratospheric warmings and their surface impacts. *Geophys. Res. Lett.* **46**, 10578–10588 (2019).
25. Waugh, D. W. Persistence of the lower stratospheric polar vortices,. *J. Geophys. Res.* **104**, 27191–27201 (1999).
26. Waugh, D. W. Interannual variability in the decay of lower stratospheric Arctic vortices. *J. Met. Soc. Jpn.* **80**, 997–1012 (2002).
27. Black, R. X., McDaniel, B. A. & Robinson, W. A. Stratosphere-troposphere coupling during spring onset. *J. Climate* **19**, 4891–4901 (2006).
28. Black, R. X. & McDaniel, B. A. The dynamics of the Northern Hemisphere Stratospheric Final Warming event. *J. Atmos. Sci.,* **64**, 2932–2946 (2007).
29. Hersbach, H. et al. The ERA5 global reanalysis. *Q. J. R. Meteorol. Soc.* **146**, 1999–2040 (2020).
30. Butler, A. H. & Domeisen I. V. The wave geometry of final stratospheric warming events. *Weather Clim. Dyn.* (under review) https://doi.org/10.5194/wcd-2020-63 (2021).
31. Newman, P. A. & Nash, E. R. Quantifying the wave driving of the stratosphere, *J. Geophys. Res.* **105**, 12485–12497 (2000).
32. Simmons, A. et al. Global stratospheric temperature bias and other stratospheric aspects of ERA5 and ERA5.1. *ECMWF Technical Memorenda* N° 859, 01/2020, https://www.ecmwf.int/sites/default/files/elibrary/2020/19362-global-stratospheric-temperature-bias-and-other-stratospheric-aspects-era5-and-era51.pdf (2020).

Acknowledgements

This work was supported by Centre National de la Recherche Scientifique, UVSQ Université Paris-Saclay and Sorbonne Université and the project Atmospheric dynamics Research InfraStructure Project (ARISE 2) funded by the European Union's Horizon 2020 Research and Innovation programme under grant agreement n° 653980. The ERA5 data are provided by ECMWF Copernicus Climate Change Service from their data server https://cds.climate.copernicus.eu/cdsapp#!/dataset/reanalysis-era5-pressure-levels?tab=form.

Author contributions

Alain Hauchecorne developed and applied the methods of analysis of ERA5 data, interpreted the results and wrote most of the paper. Chantal Claud and Philippe Keckhut participated to the conception of the study, the interpretation of the results and the writing of the paper. Alexis Mariaccia participated to the analysis of the results.

Competing interests

The authors declare no competing interests.

Additional information

Supplementary information The online version contains supplementary material available at https://doi.org/10.1038/s43247-021-00335-z.

Correspondence and requests for materials should be addressed to Alain Hauchecorne.

Peer review information *Communications Earth & Environment* thanks the anonymous reviewers for their contribution to the peer review of this work. Primary Handling Editor: Heike Langenberg. Peer reviewer reports are available.

Reprints and permission information is available at http://www.nature.com/reprints

Publisher's note Springer Nature remains neutral with regard to jurisdictional claims in published maps and institutional affiliations.

Open Access This article is licensed under a Creative Commons Attribution 4.0 International License, which permits use, sharing, adaptation, distribution and reproduction in any medium or format, as long as you give appropriate credit to the original author(s) and the source, provide a link to the Creative Commons license, and indicate if changes were made. The images or other third party material in this article are included in the article's Creative Commons license, unless indicated otherwise in a credit line to the material. If material is not included in the article's Creative Commons license and your intended use is not permitted by statutory regulation or exceeds the permitted use, you will need to obtain permission directly from the copyright holder. To view a copy of this license, visit http://creativecommons.org/licenses/by/4.0/.

© The Author(s) 2022